



Path Planning Improvement for Wheel-Legged Lunar Rovers Based on Fuzzy Control and Ant Colony Optimization

Feiyang Zhang

School of Mechatronics and Vehicle Engineering, Chongqing Jiaotong University, Chongqing, 400074, China

ZHANG1001202508@outlook.com

Abstract. Path planning constitutes one of the fundamental technologies in robotic navigation. Focusing on the operational environment of wheel-legged lunar rovers on the actual lunar surface, this paper proposes and establishes a novel integrated planning methodology based on fuzzy control theory and ant colony optimization (ACO). First, based on terrain feature weights extracted from actual lunar surface scan data, we construct a three-dimensional lunar terrain model using PyCharm Matplotlib that accurately represents these characteristics. The performance parameters and constraints of the lunar rover are then systematically defined. Subsequently, we implement targeted improvements to the conventional ant colony optimization (ACO) algorithm based on actual operational conditions. A fuzzy logic controller is designed with an empirically initialized rule base, culminating in a novel hybrid control algorithm. Subsequently, the proposed algorithm was implemented in the 3D lunar terrain model. Simulation experiments were conducted under specified parameters and constraints, with comparative testing against both the A* algorithm and the genetic algorithm (GA). Results demonstrate that after 100 iterations, our method outperforms the benchmark algorithms in multiple performance metrics, including path optimality, response speed, and obstacle avoidance success rate, confirming its superior effectiveness and efficiency in lunar surface environments.

Keywords: Fuzzy Control, Ant Colony Optimization, PyCharm, Path Planning, Wheel-Legged Lunar Rover.

1 Introduction

With the continuous advancement of deep space exploration, all-terrain rovers have gradually emerged as a research hot spot. Among these, wheel-legged robotic explorers have gained widespread application across multiple domains due to their combined advantages of both wheeled and legged mobile robots. To enhance the efficiency of wheel-legged robots in exploring unknown and complex terrains breakthroughs and optimizations in the core technical challenges of path planning have become a critical research focus. To address the path planning challenges for

wheel-legged lunar rovers in lunar exploration missions, the path planning system must achieve precise, rapid, and highly efficient autonomous navigation across complex terrains such as craters and rocky obstacles. Additionally, it must simultaneously satisfy multiple critical requirements:

In recent research, the domestic approach predominantly features Shanghai Jiao Tong University's Configuration Topology-Extended MDp path planning system. This system employs GF sets to construct configuration topology sequences, quantitatively evaluates energy consumption for all motions of wheel-legged robots and predicts navigation risks, performs hierarchical optimization to reduce computational load, and ultimately determines optimal path selections [1]. An impedance-posture coordinated controller was concurrently designed to ensure stability during wheel-leg mode transitions [2]. However, this planning approach still exhibits limitations, including real-time performance constraints, insufficient multi-objective integration, and weak terrain generalization capability.

Internationally, the mainstream approach is the 'Neural-Differential Flatness' hierarchical planning system [3]. Targeting dynamic obstacle avoidance capability of wheel-legged robots in complex environments, it builds differential flatness models by introducing pseudo-arc mapping techniques based on stability networks, enabling adaptation to variable terrains [4]. However, it still relies on static environment maps, shows low real-time dynamic obstacle avoidance efficiency, and heavily depends on GPU computing power of front-end neural networks [5].

Regarding the existing shortcomings in current path planning systems concerning dynamic obstacle avoidance capability, terrain adaptability, and computational efficiency, this paper proposes a novel path planning method that integrates fuzzy control theory with ant colony optimization (ACO). Based on actual lunar terrain data, we designed a fuzzy controller and established a corresponding fuzzy rule base to achieve dynamic adjustment of process parameters, thereby enhancing the algorithm's dynamic adaptability and real-time obstacle avoidance capability in complex terrains. This novel path planning method demonstrates significant advantages over conventional approaches in global optimum path searching, computation time, and obstacle avoidance success rate, proving more effective in meeting the practical requirements for path planning in complex lunar surface environments.

2 The Establishment of Theoretical Models Based on Practical Problems

Through the analysis and synthesis of conventional optimization algorithms (including the ant colony algorithm in this study), we identify their prevalent limitations: susceptibility to local optima, reliance on explicit modeling, and poor dynamic adaptability [6]. To address these limitations, this study proposes an enhanced ant colony optimization (ACO) algorithm that integrates fuzzy control theory. The improved algorithm has been specifically designed and optimized to meet the practical requirements of wheel-legged lunar rover exploration on the lunar

surface.

2.1 Terrain Modeling

This study utilizes actual lunar surface scan data provided by the Yutu rover to analyze its data characteristics and weight distribution. Using PyCharm, we generated a realistic $30\text{m} \times 30\text{m}$ 3D model that accurately represents lunar terrain features, as shown in Fig.1. This model serves as the practical application scenario for subsequent algorithm simulations, enabling feasibility verification of the improved algorithm.

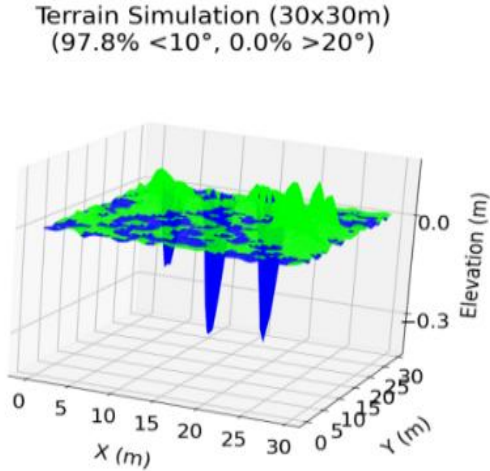


Fig. 1. 3D lunar surface grid map.

The following explains key lunar terrain characteristics:

- (1) The lunar terrain exhibits predominantly gentle slopes. Slope characteristics typically remain below 10° , with rare craters potentially reaching 20° .
- (2) Crater Characteristics, based on scan data, the craters exhibit diameters ranging from 1 to 10 meters, with a depth-to-diameter ratio of approximately 1:8, predominantly comprising shallow depressions.
- (3) For lunar surface obstacles, the height and width ranges are 0.1-0.5 m and 0.5-2 m, respectively. Within a $30\text{ m} \times 30\text{ m}$ area, the number of obstacles is approximately 4 to 19.

2.2 Parameters and Constraints of Wheel-Legged Lunar Rover

Reference to the performance parameters of existing lunar rover locomotion mechanisms and payload systems, parameter values and constraints for subsequent simulation calculations are established as presented in Table 1.

Table 1. Parameters and constraints of the wheel-legged lunar rover

Parameter name	Parameter value
Wheel motion space sector radius	0.3 m
Wheel motion space sector central angle	120°
Maximum robot movement speed	0.5 m/s
Maximum robot motion acceleration	0.1 m ² /s
Minimum turning radius of the robot	1 m
Minimum safety distance	0.2 m
Maximum obstacle-crossing height	0.3 m
Legged locomotion speed	0.3 m/s

Supplementary note: The mode-switching threshold for the wheel-legged lunar rover is set as follows: wheeled mode is employed when the slope is $<5^\circ$, while legged mode is activated when the slope exceeds $>5^\circ$ or when obstacle crossing is required below the leg-lifting limit height [7].

2.3 Improvements Based on the Classical Ant Colony Algorithm Model

Before designing the fuzzy controller, to better adapt it to fuzzy control rules, this study proposes an improved fitness function-based pheromone update mechanism for the classical ant colony algorithm, specifically for three-dimensional complex terrains. This modification enhances the algorithm's compatibility with fuzzy control systems.

For actual three-dimensional lunar terrain, if an initially planned path has length L and smoothness S , its adaptive function is given by Equation (1):

$$C = w_1 \cdot L + w_2 \cdot S \quad (1)$$

Where w_1 and w_2 are the weighting factors for path length and smoothness, respectively, L denotes the total path length [8]:

$$L = \sum_{i=2}^{N-1} \sqrt{(x_{i+1} - x_i)^2 + (y_{i+1} - y_i)^2 + (z_{i+1} - z_i)^2} \quad (2)$$

Where (x_i, y_i, z_i) and $(x_{i+1}, y_{i+1}, z_{i+1})$ respectively represent the coordinates of the current node and the next node in the three-dimensional terrain map along the path formed during ant colony dispersal.

Smoothness S can be expressed by Equation (3)

$$S = \frac{1}{N-2} \sum_{i=2}^{N-1} (\theta_{h,i} + \theta_{v,i}) \quad (3)$$

Where θ represents the horizontal rotation angle and vertical rotation angle, respectively.

When the ant colony completes an iteration, the fitness function from the previous iteration will be replaced with the new one, and the pheromone levels at each node are updated as shown in Equation (4) [9].

$$\Delta \tau_i^k = \begin{cases} \frac{Q}{c}, & \text{If ant } k \text{ traverses between locations } i \text{ and } j \\ 0, & \text{Others} \end{cases} \quad (4)$$

where Q denotes the pheromone constant and C represents the fitness function.

The updated mechanism enhances the ant colony's iterative process by enabling redundant path pruning from previous iterations, thereby strengthening the exploration of high-quality paths while effectively reducing computation time.

3 Construction of the Fuzzy Controller

3.1 Principles of Fuzzy Control

For complex control objects, operations are described based on empirical knowledge and human linguistic rules. Sensor measurements then determine parameter thresholds, enabling fuzzy representation of the problem, which is ultimately defuzzified to generate output control signals. This paper summarizes the principles as shown in Fig.2.

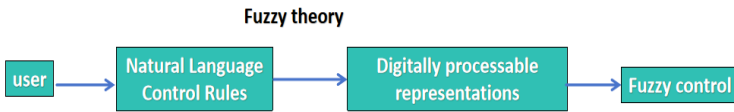


Fig. 2. Fuzzy Control Principle.

3.2 Principle of Fuzzy Controller

For specific problems, targeted parameters and fuzzy linguistic rules are established based on empirical knowledge. Through iterative refinement, a fuzzy rule control library denoted as the knowledge base in Fig.3 is developed and perfected.

First, the schematic diagram of the fuzzy controller is presented, as shown in Fig.3.

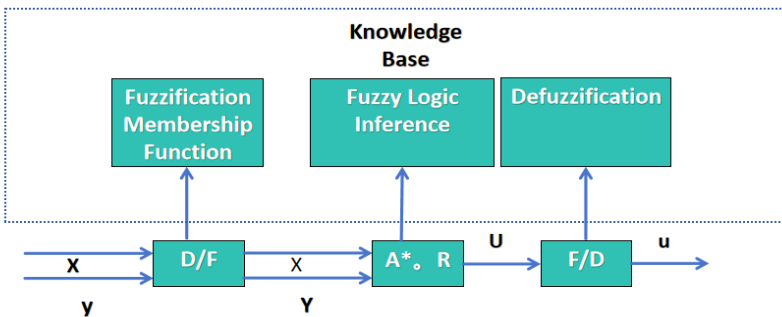


Fig. 3. Schematic diagram of the fuzzy controller.

3.3 Design of the Fuzzy Controller Based on the Ant Colony Algorithm

First, preliminary design of the controller is conducted based on the actual working environment of the wheel-legged lunar rover and the initially improved ant colony algorithm, with the fuzzy linguistic rules defined as follows:

- (1) Input: Terrain complexity (S), Distance (D)
Output: Pheromone evaporation coefficient (ρ), Heuristic factor (β)
- (2) The terrain complexity is defined using three fuzzy linguistic descriptors - Low (L), Medium (M), and High (H)- which are formulated as three fuzzy sets.
- (3) The target distance is characterized by three fuzzy linguistic descriptors - Near (N), Medium (M), and Far (F)- constituting three fuzzy sets.

Guided by fuzzy control principles, the pheromone evaporation coefficient (ρ) and heuristic factor (B) output by the ant colony algorithm are further optimized and expressed as follows:

$$\tau_{ij}(t+1) = (1 - \rho)\tau_{ij}(t) + \sum_{k=1}^m \Delta\tau_{ij}^k \tag{5}$$

Subsequently, based on lunar surface exploration experience and practical operational knowledge of the wheel-legged lunar rover, seven fuzzy control rules were initially formulated to establish a fuzzy rule control library. The specific implementation is presented in the simulation section.

4 Simulation and Results Analysis

4.1 Preliminary Verification and Simulation Results

To preliminarily validate the feasibility of the novel path planning method integrating fuzzy control with the ant colony algorithm, this paper first simplifies the model.

Within the PyCharm environment, a 100×100 planar search area was established, with 40 randomly generated coordinate points serving as search targets under given threshold conditions, along with designated start and end points. The new planning algorithm was then imported and executed, visualizing the globally optimal path as shown in Fig.4.

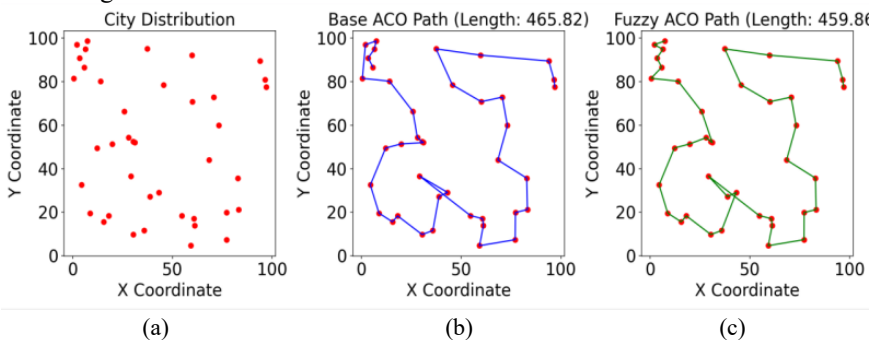


Fig. 4. Path planning in a 2D plane: (a) target point; (b) base ACO path; (c) fuzzy ACO path.

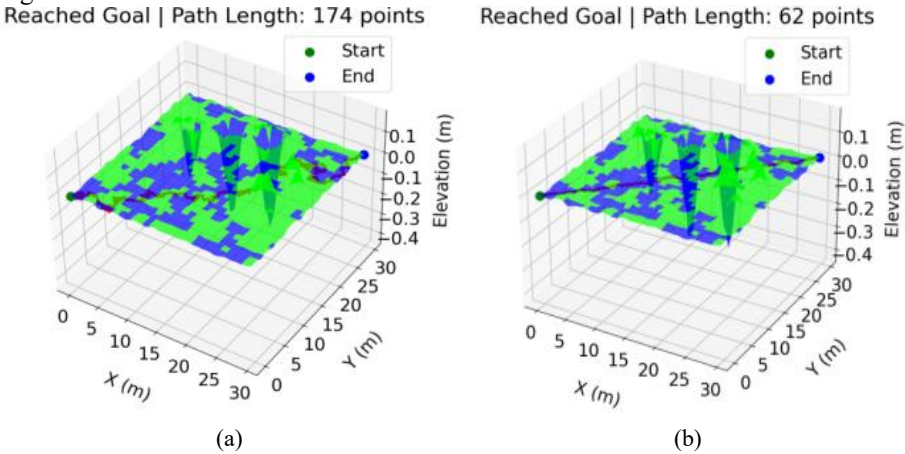
Please note that the first paragraph of a section or subsection is not indented. The first paragraphs that follow a table, figure, equation, etc., do not have an indent.

First, it is explicitly defined that the path starts at the upper-left corner and terminates at the upper-right corner.

As shown in the figures, Fig.4 (a) displays the target points to be searched by the robot, Fig.4 (b) presents the path planned by the conventional ant colony algorithm with a length of 465.82, Fig.4 (c) shows the path generated by the new planning algorithm, measuring 459.86 in length Comparative analysis between Fig.4 (b) and Fig.4 (c) reveals distinct initial search path variations in the upper-left corner. The results demonstrate that incorporating fuzzy control effectively mitigates the conventional ant colony algorithm's tendency to converge on local optima due to excessive initial pheromone concentration, thereby significantly improving the probability of discovering globally optimal paths.

4.2 Path Planning and Algorithm Comparison Based on Actual Lunar Surface Characteristics

Following the preliminary validation of the algorithm's feasibility in Section 3.1, this section implements the integrated algorithm and initially establishes a fuzzy rule library into the 3D grid map (generated in Section 2.1) that accurately reflects actual lunar terrain characteristics. The planning of the wheel-legged lunar rover operates under all constraints specified in Table 2, while concurrently incorporating existing improved genetic algorithms and A* algorithms. With predefined start and end points, the rover autonomously navigates and plans paths across the lunar surface. Finally, PyCharm-based path planning simulations are conducted, with results visualized in Fig.5.



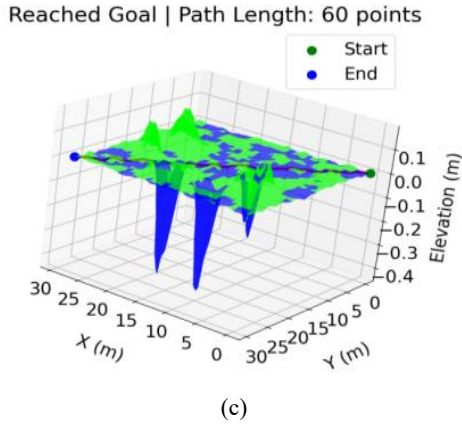


Fig. 5. Performance comparison of GA, A*, and hybrid algorithms: (a) GA path; (b) A* path; (c) fuzzy ACO path.

Fig.5 (a)-5 (c) respectively present the simulation results of the GA, A*, and hybrid algorithms implemented on the 3D terrain map with actual lunar surface characteristics. As demonstrated in the figures, the proposed hybrid algorithm achieves superior path planning performance on actual lunar terrain (Fig.5 (c)), with a total path length of 62 units, significantly outperforming the other two algorithms in trajectory optimization. GA Subsequent paragraphs, however, are indented. The GA algorithm (Fig.5 (a)) yields a path length of 164 units and becomes trapped in local optima for an extended period during its mid-to-late stage. The A* algorithm (Fig. 5 (b))demonstrates relatively better performance with a path length of 68 units, though it has an obstacle. Crossing calculations still exhibit precision deficiencies due to the absence of a dedicated rule library tailored for this specific problem category.

Similarly, to obtain comprehensive algorithmic performance data, subsequent tests conducted 100 iterations for each of the three algorithms, the other two benchmark algorithms are the A* and Genetic Algorithm (GA), both implemented based on established research [10, 11]. With comparative metrics (average planning time and obstacle avoidance success rate) summarized in Table 2.

Table 2. Performance comparison of algorithms

Algorithm	Path length (m)	Planning time (s)	Obstacle avoidance success rate (%)
GA	174	1.23	89%
A*	62	0.87	92%
The proposed algorithm	60	0.76	98%

As clearly evidenced in Table 2, the proposed hybrid algorithm integrating ant colony optimization and fuzzy control demonstrates superior performance. Specifically adapted for wheel-legged lunar rovers operating on actual lunar terrain through empirically established fuzzy rule libraries, it achieves shorter computation

time, higher obstacle avoidance success rate, and reduced path length-confirming both the feasibility and advantages of this integrated approach.

5 Conclusion

With the rapid development of deep space exploration, addressing path planning challenges for wheel-legged lunar rovers under actual lunar surface conditions has become critically significant. This paper proposes an improved path planning algorithm integrating ant colony optimization with fuzzy control, validated through 3D grid maps simulating realistic lunar terrain features, with comparative analysis against other mainstream algorithms. The results demonstrate that the proposed algorithm exhibits superior adaptability to such practical challenges, achieving significant optimization in computational efficiency, obstacle avoidance success rate, and optimal path length. The improved algorithm constructs targeted fuzzy controllers and rule libraries for specific problems, overcoming limitations of traditional explicit modeling approaches by resolving issues like local optima convergence, prolonged computation time, and poor adaptability to complex environments-demonstrating strong application potential.

References

1. Yuan, S.: Motion planning and control of a six-Legged wheel-legged robot on lunar surface. Nanjing University of Aeronautics and Astronautics, Nanjing, China (2019).
2. Fusco, G.: Motion planning of differentially flat Planar Underactuated Robots. *Mechanical Science and Technology* 43 (3), 57-66 (2024).
3. Wang, K., Wu, X., Shi, S.: A novel integrated path planning and mode decision algorithm for wheel-leg vehicles in unstructured environment. *Sensors* 25(9), 1888-1888 (2025).
4. Sun, J., Sun, Z., Wei, P.: Path planning algorithm for a wheel-legged robot based on the theta* and timed elastic band algorithms. *Symmetry*, 15(5), 1-25 (2023).
5. Kim, S., Jang, H., Ha, J., et al.: Efficient graph-based multi-story path planning with optimized elevator selection for indoor delivery robots. *Electronics* 14(5), 982-982 (2025).
6. Shuaiyong, L., Jingwen, H., Wenping, M., et al.: A path planning algorithm for mobile robots in dynamic environments 48(3), 245-261 (2025).
7. Mei, X., Wei, Y., Guo, C., Zhang, X.: Experimental research of wheel-legged robot crossing obstacles. *Robotica* 43(7), 2459-2479 (2025).
8. Balootaki, A., M., Rahmani, H., Moeinkhah, H., et al.: A new predictive intelligent controller and path planning for mobile robots. *Journal of Vibration and Control* 31(9-10), 1667-1678 (2025).
9. Fan, W., Liao, Z., Bai, Y.: Improved ACO algorithm fused with improved Q-Learning algorithm for besse curve global path planning of search and rescue robots. *Robotics and Autonomous Systems* 182, 104822-104822 (2024).
10. Li, Z., Shi, R., Zhang, Z.: A new path planning method based on sparse A* algorithm with map segmentation. *Transactions of the Institute of Measurement and Control* 44(4), 916-925 (2025).

11. Xu, H., Niu, Z., Jiang, B., Zhang, Y., Chen, S., Li, Z., Gao, M., Zhu, M.: ERRT-GA: Expert genetic algorithm with rapidly exploring random tree initialization for multi-UAV path planning. *Drones* 8(8), 367-367 (2024).

Open Access This chapter is licensed under the terms of the Creative Commons Attribution-NonCommercial 4.0 International License (<http://creativecommons.org/licenses/by-nc/4.0/>), which permits any noncommercial use, sharing, adaptation, distribution and reproduction in any medium or format, as long as you give appropriate credit to the original author(s) and the source, provide a link to the Creative Commons license and indicate if changes were made.

The images or other third party material in this chapter are included in the chapter's Creative Commons license, unless indicated otherwise in a credit line to the material. If material is not included in the chapter's Creative Commons license and your intended use is not permitted by statutory regulation or exceeds the permitted use, you will need to obtain permission directly from the copyright holder.

